Atmospheric Research 290 (2023) 106799

Contents lists available at ScienceDirect

Atmospheric Research

journal homepage: www.elsevier.com/locate/atmosres

Lagged compound dry and wet spells in Northwest North America under 1.5 °C–4 °C global warming levels

Reza Rezvani [a], Wooyoung Na [a,b], Mohammad Reza Najafi [a,*]

[a] Department of Civil and Environmental Engineering, Western University, London, Ontario N6A 5B9, Canada
[b] Department of Civil Engineering, Dong-A University, Busan 49315, Korea

ARTICLE INFO

Keywords:
Climate change
Compound wet and dry spells
Multi-model ensemble
Dry-wet abrupt alternation
Compound extreme events
Northwest North America

ABSTRACT

The increasing variability and rapid transitions between hydroclimatic extremes and their compounding economic and environmental effects can cause severe consequences. Understanding the changing characteristics of such transitions, including their spatiotemporal frequency and magnitude is critical to developing effective mitigation and adaptation strategies. In this study, lagged compound dry and wet spells are investigated in Northwest North America (NWNA) based on the Standardised Precipitation Index and Standardised Precipitation Evapotranspiration Index for multiple accumulation periods (1, 3, and 6 months). The indices are estimated based on six downscaled Global Climate Models that participated in the 5th phase of the Coupled Model Intercomparison Project under the Representative Concentration Pathways (RCPs) 4.5 and 8.5, in addition to the Variable Infiltration Capacity hydrologic model simulations. We characterize changing behaviour of the lagged compound dry and wet spells under 1.5 °C–4 °C global warming levels. Projections show overall increases in the frequency of wet and dry swings and decreases in the corresponding transition times in NWNA under climate change. In addition, the magnitude, intensity, and duration of wet and dry components of such lagged compound events are projected to increase. With some differences, both indices identify the entire Columbia and southern Fraser basins as hotspots for frequent compound event occurrences. The study identifies increasing hotspots across the domain affected by abrupt transitions under climate change and asserts the necessity of integrating mitigation measures targeting such lagged compound events into disaster risk reduction strategies.

1. Introduction

Hydroclimatic extremes (i.e., floods and droughts) occur globally and frequently and their occurrence is not confined to a specific geographical location (Van Loon, 2013). Floods are mainly triggered by persistent and widespread wet spells (He and Sheffield, 2020), while droughts arise from prolonged periods of abnormally low precipitation also known as dry spells (Van Loon, 2015). Floods can occur fast at any time of the year, often having visible, and dramatic social, economic, and environmental consequences. On the contrary, droughts have a much larger spatial and temporal scale and can impact freshwater ecosystems and their inhabitants, limiting hydropower generation, drinking water supply, crop production, and waterborne transportation (Van Loon, 2013). Moreover, hydroclimatic extremes are expected to become more variable due to anthropogenic climate change (Chen and Wang, 2022). There is growing evidence that climate change can lead to increases in the frequency and intensity of hydrologic extremes (He, 2019; Hirabayashi et al., 2013; Herring et al., 2015). For instance, rising global temperatures can increase the concentrations of atmospheric moisture due to increased evaporation and transpiration. Moreover, the water-holding capacity of the atmosphere can expand according to the Clausius-Clapeyron relation (Skliris et al., 2016). Increasing atmospheric water content and its water-holding capacity can collectively lead to more extreme precipitation events that can translate into more severe flooding (Garcia et al., 2022; He and Sheffield, 2020; Bush and Lemmen, 2019). In addition, global warming induced increase in evapotranspiration can lead to prolonged and more frequent drought occurrences if the moisture deficits from increased evapotranspiration are not offset by the precipitation increases (He and Sheffield, 2020; Bush and Lemmen, 2019).

Complex interactions between various physical processes can cause weather and climate-related extreme events (such as droughts, floods, heatwaves, and storms), which can overwhelm the capacity of natural and human systems to cope with, and create societal or ecological

* Corresponding author.
E-mail address: mnajafi7@uwo.ca (M.R. Najafi).

https://doi.org/10.1016/j.atmosres.2023.106799
Received 24 December 2022; Received in revised form 27 April 2023; Accepted 4 May 2023
Available online 9 May 2023

impacts (Singh et al., 2020, 2021, 2022; Zscheischler et al., 2020). The combination of multiple drivers and/or hazards (which may not necessarily be extreme) can amplify the impacts of individual event occurrences, which is referred to as compound extreme events (Leonard et al., 2014). The impacts of hazards in compound events are owing to a) multiple hazards occurring simultaneously at one location (e.g., pluvial and coastal flooding); b) hazards occurring concurrently in different locations (e.g., flooding in several locations in an area); c) hazard(s) exacerbating impacts of a pre-existing hazard (e.g., heatwave during a drought); and d) temporal succession of hazards (e.g., successive floods and droughts) (Zscheischler et al., 2020). Since the introduction of compound events in the Intergovernmental Panel on Climate Change (IPCC) Special Report on Climate Extremes (SREX) in 2012, several compound weather and climate extremes have been investigated regionally and globally. This includes compound drought and heat waves (Mukherjee and Mishra, 2021; Zhou et al., 2019), compound flooding (Jalili Pirani and Najafi, 2020 & 2022), precipitation and temperature extremes (Singh et al., 2020) among others that concluded with the necessity of a multivariate perspective to appropriately assess changes in climate extremes and their impacts.

However, most studies on floods and droughts to date have treated the two extremes separately. Therefore, the intersection between these two extremes has been overlooked, even though their rapid transitions can lead to greater economic and environmental impacts than the sum of each type of event (He and Sheffield, 2020).

Historically, several catastrophic instances of transition between drought and flood have been recorded globally. For example, widespread floods in California in 2016–17 occurred on the back of the multi-year drought, and the drought to flood events of 2011–12 in England and Wales (Parry et al., 2013). Most recently (2021), a dry summer in British Columbia, Canada that led to several wildfires, was followed by massive flooding in the fall brought about by an atmospheric river that caused 5 fatalities and landslides (Gillett et al., 2022).

Abrupt alterations between droughts and flooding, featuring quick transitions from one extreme to the other are particularly problematic for water managers (Swain, 2015; Swain et al., 2016; Maxwell et al., 2017). Successive flood and drought events put emergency and hazard response teams under significant stress (Leonard et al., 2014), and exacerbate the tension between stressed resources for flood relief or long-term water resource management (Parry, 2019). Moreover, successive floods and droughts can impair the functionality and threaten the stability of structures used as mitigation measures such as dikes and levees (e.g., in California as documented in Vahedifard et al., 2017; Vahedifard et al., 2015), dams, and others (Ward et al., 2020).

Recent devastating occurrences of successive floods and droughts across the world, such as in Australia (Mount et al., 2017), England (Parry et al., 2013), and California (Wang et al., 2017) have ignited the motivation of studying such disastrous events. He and Sheffield (2020) studied the historical trends of drought-pluvial seesaw globally and identified several hotspots including NWNA for lagged occurrences of pluvial-drought events. Using the Palmer drought severity index (PDSI), Maxwell et al. (2013) suggested that tropical cyclones can bring about synoptic conditions favourable for drought to flood events in coastal regions of the southeastern United States. Maxwell et al. (2017) explored the changes in the mechanisms causing rapid drought-to-flood events in the southern United States and found Frontal, Tropical, and Airmass storm types during warm-season droughts can lead to rapid drought-to-flood events. Variability and transitions of contrasting precipitation extremes in the midwest United States over the past 70 years were investigated by Ford et al. (2021) using the standardised precipitation index (SPI). Ansari and Grossi (2022) used the standardised precipitation evapotranspiration index (SPEI) to study the historical spatiotemporal evolution of the features of wet-dry events and their transitions in a watershed in Asia and found hotspots for each feature of such compound events. A global study by Chen and Wang (2022) based on SPEI projected accelerated transitions between wet and dry spells under climate change. Using precipitation as an indicator, Swain et al. (2018) projected an increasing frequency of "precipitation whiplash" events over California similar to the 2016–17 event in this state.

Despite many records of the lagged compound dry-wet spells globally (Parry, 2019), only a few regional analyses have been conducted, mainly in the U.S. and China, and understanding of such events is limited. Moreover, previous studies have evaluated these events using single indicators (e.g., precipitation) or different climatic indices in isolation, and the effectiveness of different metrics in characterizing the transitions under different physiographic and hydroclimatic regimes has not been investigated. Given the expected intensification of the hydroclimatic extremes under climate change, and that areas in higher latitudes are expected to warm at a higher rate compared to the global average (Bush and Lemmen, 2019), it is important to analyze the changing behaviour of lagged compound events in these domains. To this end, we use an ensemble of downscaled CMIP5 GCM. Using a multimodel ensemble allows for identifying a range of variability in the changing characteristics of compound wet and dry events. In addition, conducting such investigation on a large basin scale can provide critical insights into the regional impacts of the lagged compound dry and wet spells under climate change, valuable to a wide range of decision-makers. Therefore, the objective of this study is to better understand how different characteristics of lagged compound dry-wet spells can change across three large basins in northwest North America in a warmer climate. In particular, we aim to answer the following questions:

- How often are lagged compound dry and wet spells expected to occur at different global warming levels?
- How long can it take for the dry and wet spell of a compound event to swing (transition time) at different global warming levels?
- Bearing in mind the projected intensification of the global hydrological cycle in a warming climate, is the study area expected to experience successions of more severe dry and wet spells? If so, to what extent are such dry and wet spells projected to intensify?
- How well can different climatic indices model the lagged compound wet and dry events?

2. Study area and data

2.1. Study area

The study area consists of three key basins of Peace, Fraser and Columbia in Northwest North America (NWNA) covering British Columbia (B.C.) and Alberta in Canada, and Washington, Montana, Oregon, and Idaho in the United States (Fig. 1). This area was selected since lagged compound dry and wet spells have previously occurred within (e.g., 2021 in British Columbia; Gillett et al., 2022) or in proximity (e.g., 2016–17 in California; Swain et al., 2018) to NWNA. Located in western Canada, the Peace River Basin (PRB) headwaters are situated in the Rocky Mountains. The PRB drains an area of approximately 101,000 km^2 and covers parts of north-central B.C. and northeastern Alberta (Vore et al., 2020; Romolo et al., 2006). The PRB is a heterogenous catchment with elevation ranging from 400 to over 2800 m and the average temperature ranging between −11.7 °C in January and 12.4 °C in July over the basin (Najafi et al., 2017). As the largest drainage basin in BC, the Fraser River Basin (FRB) is a physiographically heterogeneous catchment that drains almost 230,000km^2 from its headwaters in the Rocky Mountains (near Jasper, Alberta) to the Pacific Ocean at Vancouver (Schnorbus et al., 2010). Elevation in the FRB ranges from sea level to 4000 m. As a snow-dominated basin, the mean annual precipitation in the FRB varies between 200 and 5000 mm. The average temperature of the basin ranges from −8.9 °C in January to 13.1 °C in July (Najafi et al., 2017). The Columbia River Basin (CRB) drains an area of 560,000 km^2 and is affected by contrasting climatic regimes. The western slopes and coastal mountainous regions experience moderate temperatures and receive some of the highest

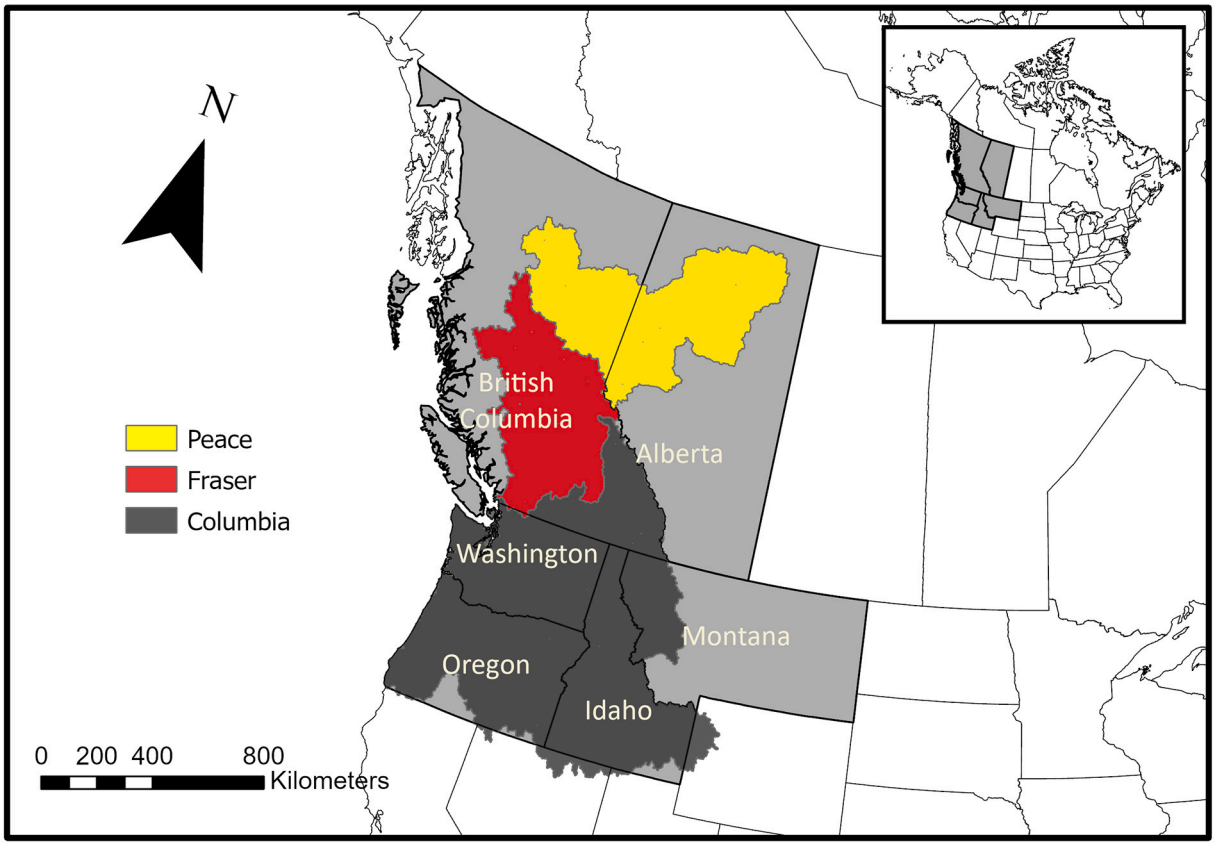

Fig. 1. Location map of Northwest North America and the three key basins considered in this study (Peace, Fraser, and Columbia).

precipitation in North America (500–750 mm near the mountain foothills and 1000 mm or more in the coastal mountains). The interior parts of the CRB receive considerably less precipitation (<200 mm in central Washington). Precipitation primarily falls during the period from October through March, while summers are relatively dry. The CRB is bounded to the east and north by the cold and moist Rocky Mountains (Chegwidden et al., 2019).

2.2. Data

The datasets used in this study are prepared and made publicly available by the Pacific Climate Impacts Consortium (PCIC). This study was conducted based on monthly records of precipitation and potential evapotranspiration using observed and simulated values. Precipitation values were obtained from multiple downscaled Global Climate Models (GCMs). In addition, we use precipitation records of the PCIC meteorology for NWNA (PNWNAmet data) (Werner et al., 2019). The PNWNAmet is developed via the trivariate thin plate spline interpolation method using a set of long-term homogenized records of high-resolution, high station density climatology as a predictor (Werner et al., 2019). This dataset provides daily gridded observations over the NWNA domain (NWNA; 40°N to 72°N and −169°W to −101°W). The PNWNAmet provides daily maximum and minimum temperatures as well as precipitation and wind speed for 1945–2012 with a spatial resolution of 1/16° (approximately 6 km). Previously, this high-resolution gridded dataset has been utilized as a target dataset for the statistical downscaling of GCMs and forcing dataset for hydrologic modeling over the NWNA (Mahmoudi et al., 2021; Dibike et al., 2021; Shrestha et al., 2019).

We conducted the study using simulated precipitation from a representative ensemble comprising 12 members, which included six models from the 5th Phase of the Coupled Model Intercomparison Project (CMIP5) (Taylor et al., 2012), under two medium and high representative concentration pathways (RCP4.5 and 8.5) radiative forcing scenarios (Moss and Intergovernmental Panel on Climate Change, 2008). GCMs were selected using the Katsavounidis–Kuo–Zhang (KKZ) algorithm (Cannon, 2015), which includes ACCESS1–0, CanESM2, CCSM4, CNRM-CM5, HadGEM2-ES, and MPI-ESM-LR (Schoeneberg and Schnorbus, 2021). The six GCMs selected for the study were chosen to represent as much of the full range of the ensemble as possible (Cannon, 2015). This selection was based on the ability of the models to capture most of the range of simulated changes in the ETCCDI climate extremes indices, which was observed in at least 90% of the CMIP5 ensemble members (Schoeneberg and Schnorbus, 2021).

The climatic simulations used in this study are statistically downscaled and bias corrected using the Bias Correction/Constructed Analogues with de-trended Quantile mapping reordering downscaling technique (BCCAQv2) (Cannon et al., 2015) and the PNWNAmet (Werner et al., 2019) as the reference meteorology. To assess the hydrologic response of the three large river basins, outputs of potential evapotranspiration from the VIC hydrologic model set up by PCIC (Schoeneberg and Schnorbus, 2021) were used. VIC is a spatially distributed macro-scale hydrologic model, which can be forced with GCM outputs and implemented over large areas. VIC model can represent the key processes such as evapotranspiration, snow accumulation, snowmelt, soil moisture and surface and subsurface runoff in the NWNA (Curry et al., 2019; Chegwidden et al., 2019; Shrestha et al., 2019 & 2021; Werner et al., 2013; Schnorbus et al., 2010). In this study, VIC was forced with the PNWNAmet and downscaled and bias-corrected GCM simulations.

3. Methodology

3.1. Dry-wet indices

Several indices have been developed to identify wet and dry climate periods and to assess their characteristics (Drumond et al., 2021). Such indices are quantitative measures that characterize wet and dry levels by incorporating one or several variables (indicators) such as precipitation and evapotranspiration into a single numerical value (Zargar et al., 2011). Characterizing wet and dry spells enables early warning and risk analysis, which in turn leads to improved preparation and contingency planning (Kchouk et al., 2022; Zargar et al., 2011). Therefore wet-dry indices are widely used to communicate the levels of wetness and dryness anomalies.

To date, many dry-wet indices have been developed and used globally with different complexities since the nature, characteristics, and impacts of wet and dry spells can vary considerably among different sectors (such as water resources managers and engineers, agricultural producers, and hydroelectric power plant operators). But, considering that a single definition of drought does not exist, no drought index meets the requirements of all (World Meteorological Organization, 2012). In this study, we consider two commonly used indices of Standardised Precipitation Index (SPI) and the Standardised Precipitation Evapotranspiration Index (SPEI). The two indices were selected since they represent the spatial patterns of events (by providing normalized measures of relative anomalies locally), are probability-based, and have a two-folded application (can characterize both wet and dry spells). This allows us to effectively assess and explore the changes in wet and dry spell characteristics over the study area on different time scales.

3.1.1. Standardised precipitation index (SPI)

McKee et al. (1993) developed the SPI, on account of the different impacts of precipitation deficits on groundwater, reservoir storage, soil moisture, snowpack, and streamflow. Precipitation is the only parameter required for calculating the SPI. SPI is normally distributed and can be used to monitor both wet and dry spells. SPI can be calculated at different time scales (accumulation periods) such as 1, 3, 6, 9, 12, and 24 months, which can provide early warning of drought and assess meteorological, agricultural, and hydrological droughts and their severity (McKee et al., 1993). Water resources planners, research institutes, and many national meteorological and hydrological services around the world use the SPI for drought monitoring (World Meteorological Organization, 2012).

The atmospheric processes including precipitation are the starting point for the development of agricultural, hydrological, and socioeconomic drought (Sheffield and Wood, 2012). Several recent studies have used precipitation to identify lagged compound events and investigate their projected characteristics (Swain et al., 2018; Madakumbura et al., 2019; Ford et al., 2021; Chen and Ford, 2023; Chen and Wang, 2022). From a technical point of view, the presence of too many zero values can distort the application of the standardised drought index approach leading to inaccurate distribution fitting or uncertain normal quantile transformation, which are the most important parts of the index estimation (McKee et al., 1993; Shukla and Wood, 2008; Vicente-Serrano et al., 2010; Stagge et al., 2015). As monthly precipitation normally does not have zero values, using SPI allows us to show spatial variability of projected compound events without any empty space.

However, the SPI is solely dependent on precipitation and does not consider other parameters that can cause or exacerbate such hydroclimatic extremes. In particular, there is no consideration of evapotranspiration, which is one of the important factors influencing the climatic water balance (Dai, 2011). Thus, the SPI can underestimate the risk of compound events as it ignores the potential impact of increasing temperature on the intensified regional water cycle. Additionally, recent studies assessing droughts have found that it is not enough to monitor only precipitation, but the variables reflecting the change in evapotranspiration should be involved (Potop, 2011; Paulo et al., 2012; Stagge et al., 2015; Labudová et al., 2017; Pei et al., 2017). Therefore, in this study the Standardised Precipitation Evapotranspiration Index (SPEI) was also used to account for the possible effects of temperature variability and temperature extremes beyond the context of global warming.

3.1.2. Standardised precipitation evapotranspiration index (SPEI)

The SPEI is developed by Vicente-Serrano et al. (2010) based on the monthly climatic water balance. The index is defined as the difference between precipitation and potential evapotranspiration (PET) at a given accumulation period. Thus, unlike the SPI which only assesses precipitation variations, the SPEI also considers the demand from evapotranspiration. SPEI captures the main impact of increased temperatures on water demand and is theoretically based on a climatic water balance. Moreover, since the temperature is considered when calculating the SPEI, this index can account for the changes in the duration and magnitude of wet and dry spells brought about by global warming.

3.1.3. Calculation of the SPI and SPEI

The SPI and SPEI are based on the probability of precipitation and climatic water balance accumulated on a given time scale. SPI quantifies the standardised deficit or surplus of precipitation over the period of interest (also known as the accumulation period), whereas SPEI is interpreted as a relative measure of surface water surplus or deficit with respect to the hydroclimate of the reference period. Computing the SPI and SPEI involves fitting a probability density function (PDF) to the precipitation totals and climatic water balance of the accumulated period and finding the cumulative probability. By applying a quantile-to-quantile normal score transformation (Eq. 1), the SPI/SPEI is then generated by transforming the cumulative probability to the standardised normal random variable (Eq. 2) with mean zero and standard deviation of one, representing the value of the SPI/SPEI.

$$y = F_Y^{-1}(f_x(x)) \tag{1}$$

where F_x (x) is the cumulative probability of the fitted distribution function to the precipitation, F_Y (y) is the standardised normal cumulative distribution function, and y is the transformed variable (here referred to as SPI/SPEI).

$$F_Y(x) = \frac{1}{\sqrt{2\pi\sigma^2}} exp\left[-\frac{(x-\mu)^2}{2\sigma^2}\right] \tag{2}$$

where $F_Y(x)$ is the PDF of normal distribution, and σ and μ are standard deviation and mean, respectively (in our case would be one and zero, respectively).

We consider the Gamma (Eq. 3) and Log-logistic (Eq. 4) distributions to fit precipitation and climatic water balance records, to find the SPI and SPEI values following the recommendations of McKee et al. (1993) and Vicente-Serrano et al., 2010), respectively. Moreover, several studies have shown that these two distributions can adequately estimate SPI and SPEI in Canada (Tam et al., 2018; Gurrapu et al., 2022). The selected distributions were fitted to the precipitation totals using the unbiased probability weighted moment (PWM) since this method does not result in biased standard deviation values (Tam et al., 2018).

$$f(x|\alpha,\beta) = \frac{x^{\alpha-1}e^{-\beta x}\beta^{\alpha}}{\Gamma(\alpha)} \tag{3}$$

where Γ(α) is the Gamma function, α and β are shape and rate parameters, and $x, \alpha, \beta > 0$.

$$f(x|\alpha,\beta) = \frac{(\beta/\alpha)\,(x/\alpha)^{\beta-1}}{\left(1+(x/\alpha)^{\beta}\right)^2} \tag{4}$$

where α and β are scale and shape parameters, respectively. In this study, monthly SPI and SPEI values at 1-, 3-, and 6-month accumulation periods are calculated (Beguería et al., 2014) considering 1970–2000 as the base period to account for the non-stationarity induced by climate change.

3.2. Definition and characteristics of compound climatic events

To represent the dry and wet spells, we use −1 and +1 thresholds for the calculated SPI and SPEI values and investigate the variability and characteristics of the compound climatic events (CCEs) with different accumulation periods. A dry (wet) period occurs when the SPI/SPEI is continuously negative (positive) and reaches an intensity of −1 (+1) or less (more), respectively. Thus, every wet/dry event has a duration defined by its beginning and end, and an intensity for each month that the event continues. A wet-to-dry (or dry-to-wet) CCE occurs when a wet (dry) period of any duration (at least one month) is followed by a dry (wet) period of any duration (at least one month). The timespan between the end of the first period (dry or wet) to the start of the second contrasting period (wet or dry) is defined as the transition time (Fig. 2). To assure the succession of wet and dry spells amplify their individual occurrence, we limit the transition time to 6 months. Abrupt transition is referred to as a transition time that is <1 month (i.e., 0 if wet and dry occur immediately after each other). The positive sum of the SPI/SPEI for all the months within a wet or dry event is considered the event's magnitude. Intensity is defined as the average SPI/SPEI value during the event and is calculated by dividing the event's magnitude by its duration. The count of the lagged compound wet and dry spells over every 10 years in each warming period of 30 years is reported as their decadal frequency at that given warming level. We explore if the future CCEs are projected to intensify under different global warming levels.

As suggested in the IPCC's sixth assessment report and several other studies (Hausfather et al., 2022; Seneviratne et al., 2012, Seneviratne et al., 2016; Seneviratne et al., 2018), we assess the regional patterns of the compound climatic events (CCEs) using the projections of relevant hydrological and climatic variables in a base period of 1970–2000, and at the global warming levels of +1.5 to +4 °C compared to the Pre-Industrial (PI) era of 1860–1900. This approach has several advantages including mirroring the policy discourse surrounding the Paris Agreement targets of 1.5 °C and "well below 2 °C." It is also largely independent of the choice of future emissions scenario (Seneviratne et al., 2016; Seneviratne et al., 2018; Hirsch et al., 2017; Cannon et al., 2015). The global warming periods for every ensemble member are presented in Table S1.

4. Results

4.1. Increasing frequency of compound climatic events

The frequency of compound climatic events (CCEs) for the three accumulation periods of 1-, 3-, and 6 months are presented in Figs. 3 and 4 based on SPI and SPEI, respectively. The frequency of CCEs were calculated at every grid of each ensemble member over the given warming period. Then the multi-model average was calculated by averaging the spatial mean of frequency simulated by each ensemble member. As an indicator of inter-model agreement, the multi-model standard deviation of spatial means was also calculated. The bars in Figs. 3 and 4 show the multi-model average spatial mean at different warming levels. The error bars represent the standard deviation of the multi-model ensemble at each global warming level (see Fig. S1 and S2 for the spatial variation of the gridded ensemble mean).

The two drought indices consistently indicate that the frequency of CCEs with different transition times is projected to increase under climate change in all accumulation periods. However, the change of frequency is not even based on different indices, and for different transition times and accumulation periods. The number of CCE occurrences captured by the indices is smaller at longer accumulation periods. This is because longer accumulation periods tend to vary less and therefore better show the overall pattern of the CCE frequency in the study area. The two indices consistently indicate that the study area is more prone to dry-to-wet CCEs. A comparison between transition times reveals that dry-to-wet CCEs occur more swiftly compared to wet-to-dry events since the dry-to-wet events that swing within one or 3 months tend to make up a larger portion of all compound events compared to

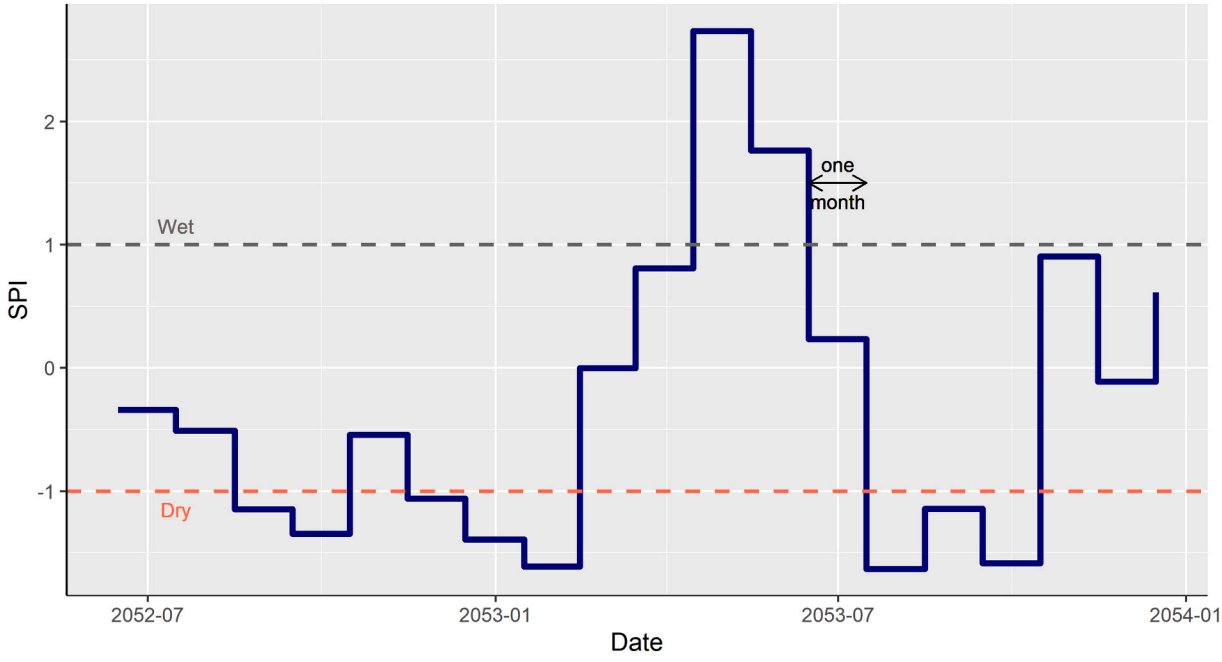

Fig. 2. Example of a compound climatic event (CCE, wet-to-dry). The blue line shows the SPI3 timeseries, while the orange and grey dashed lines illustrate the thresholds used for dry and wet conditions. Here, the transition time of the wet-to-dry CCE is one month (time span between the end of the former and the start of the latter event). (For interpretation of the references to colour in this figure legend, the reader is referred to the web version of this article.)

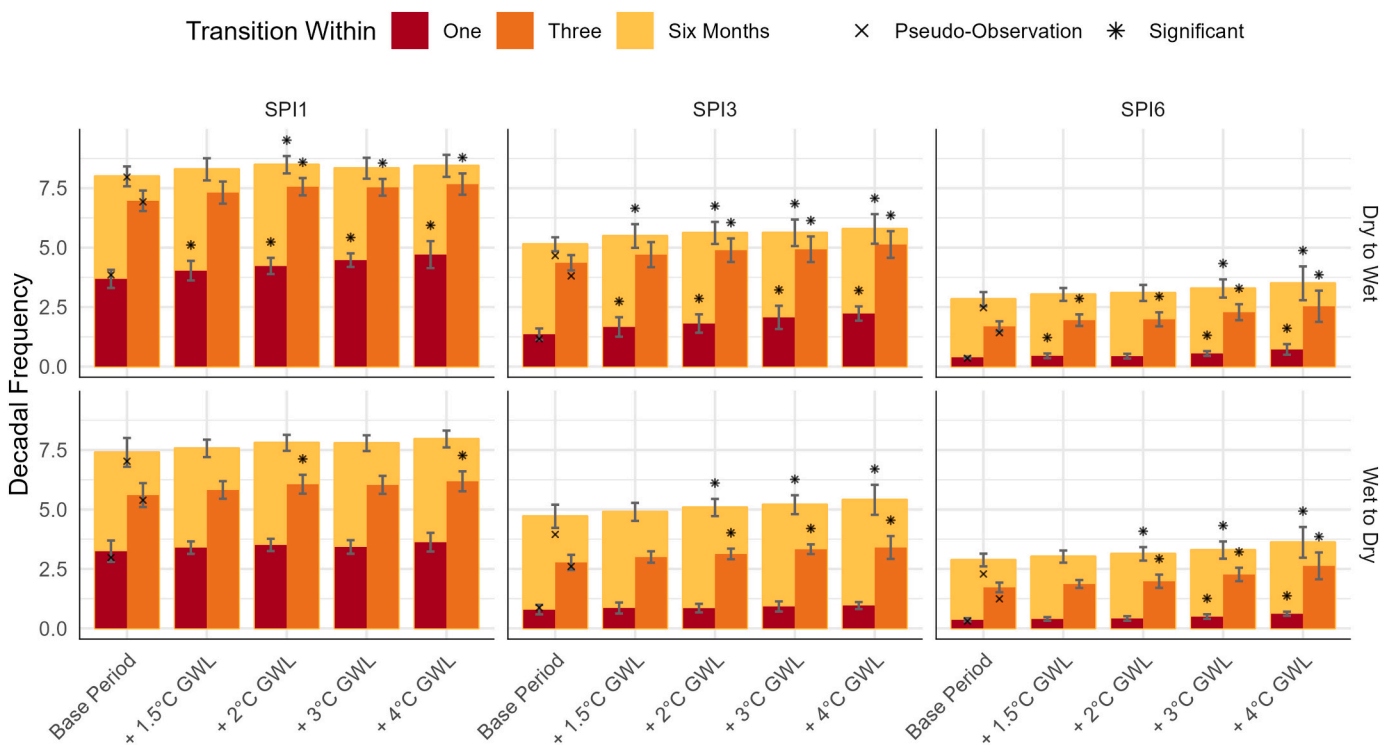

Fig. 3. Decadal frequency of CCES based on SPI. The bars show the multi-model average spatial mean of the frequency for multiple CCEs at different warming levels and accumulation periods. The error bars represent the ensemble standard deviation (± standard deviation). The bars are colored based on the transition time (yellow: within 6 months; orange: within 3 months; and red: within 1 month). (For interpretation of the references to colour in this figure legend, the reader is referred to the web version of this article.)

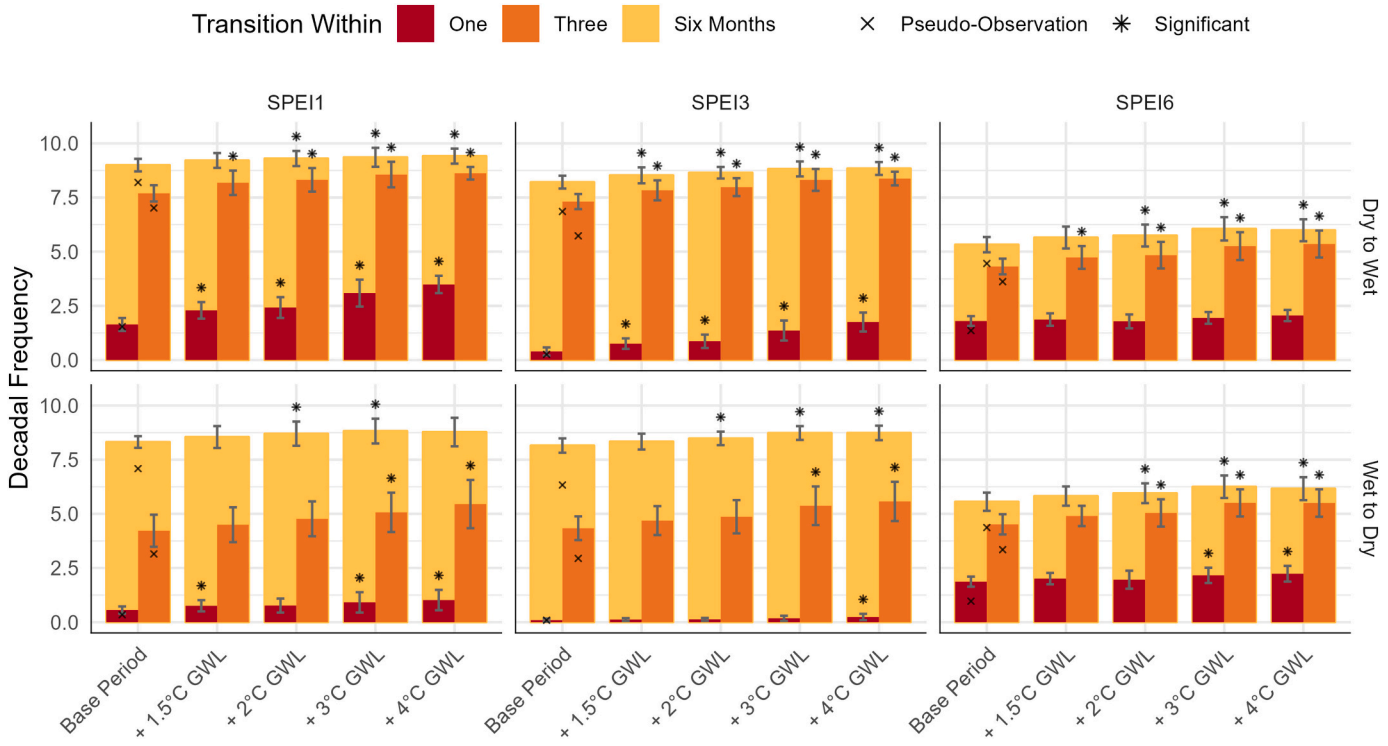

Fig. 4. Similar to Fig. 3, but for SPEI.

wet-to-dry events with the same transition time. Moreover, most dry-to-wet CCEs (more than two third of all compound events) occur within 3 months, whereas wet-to-dry events with a transition time of 3 months or less consist of almost half of all compound events (except based on SPI1 and SPEI6). In addition, abrupt dry-to-wet CCEs are projected to occur more frequently than abrupt wet-to-dry CCEs. Although the future

projections of CCE frequency based on SPI and SPEI indicate similar patterns (more frequent occurrences if warming is not limited), the number of compound events captured by SPEI is larger compared to SPI.

The results of the multi-model ensemble mean for the frequency of dry-to-wet CCEs based on SPI6 and SPEI6 are presented in maps of Figs. 5 and 6, respectively. Although the identified hotspots by the indices have similarities in the base period, there are discrepancies in the location of the future hotspots for the frequency of CCEs projected by the two indices. SPI6 identifies the entire Columbia and Fraser (except a small portion on its western boundary) basin as well as the western Peace as hotspots for frequent dry-to-wet CCE occurrence in a warmer climate (Fig. 5). On the contrary, future projections of dry-to-wet CCEs suggest the frequency of such compound events would decrease in eastern Peace and western Fraser basins at higher levels of global warming (Fig. 5). With some differences in the frequency of the CCEs, there are general agreements in the identified hot and cold spots by SPI1 and SPI3 (Figs. S3 and S4). Additionally, SPEI6 results identify the central and southeast Columbia basin as hotspots for dry-to-wet CCEs in the base period. However, the future projections indicate that under climate change, dry-to-wet CCEs can occur more frequently across the entire study area (except in central and southeast Columbia, that are hotspots in the base period). Therefore, the area is projected to experience more CCEs in a warming world. In line with the SPEI6, results based on SPEI1 and SPEI3 also show similar spatial patterns (Figs. S6 and S7). A comparison between the two indices reveals that the SPI can underestimate CCE occurrences by >2 events in some locations.

4.2. Longer compound Dry and Wet Spells with shorter transition Times

The duration of wet and dry spells and the transition time of CCEs at different warming levels are presented in Figs. 7 and 8 based on SPI and SPEI, respectively. The durations and transition times were calculated at every grid of each ensemble member over the given warming period. Then the multi-model average was calculated by averaging the spatial mean of transition time and durations simulated by each ensemble member. The points in Figs. 7 and 8 show the multi-model average spatial mean at different warming levels and the bars represent the standard deviation of the multi-model ensemble at each global warming level (see Fig. S9 and S10 for the spatial variation of the gridded ensemble mean).

When comparing dry-to-wet and wet-to-dry CCEs, the duration of wet and dry spells in both types of CCEs are almost identical at each warming level and accumulation period (based on both SPI and SPEI in Figs. 7 and 8). However, the SPI suggests that the duration of wet spells in CCEs is projected to increase. Generally, dry-to-wet CCEs based on SPI have shorter transition times compared to wet-to-dry events. In addition, the transition time is projected to significantly decrease at a higher level of global warming (Fig. 7). When considering CCEs based on SPEI, the duration of dry spells is projected to increase at higher global warming levels. A comparison between the different types of CCEs (wet-to-dry and dry-to-wet) reveals that generally, the transition time of dry-to-wet CCEs is shorter than wet-to-dry events. Furthermore, both types of CCEs are projected to occur more swiftly under global warming, which is inferred from the projected decreasing transition times if warming continues.

The climatology of transition time for dry-to-wet CCEs based on SPI6 and SPEI6 are presented in Figs. 9 and 10, respectively. Since the drought indices used in this study (SPI and SPEI) are calculated monthly and the 6 months limit is applied to transition time, the transition time of the CCEs would vary in the range of 0 to 6 months (transition time of 0 indicates that wet and dry spells occur successively with no lag between them).

The transition time of CCEs is projected to decrease under climate change across the study area with some locations excepted. While results based on SPI6 indicate that it is projected to take 3 months for dry spells to swing to wet spells across most of the study area, transition time in

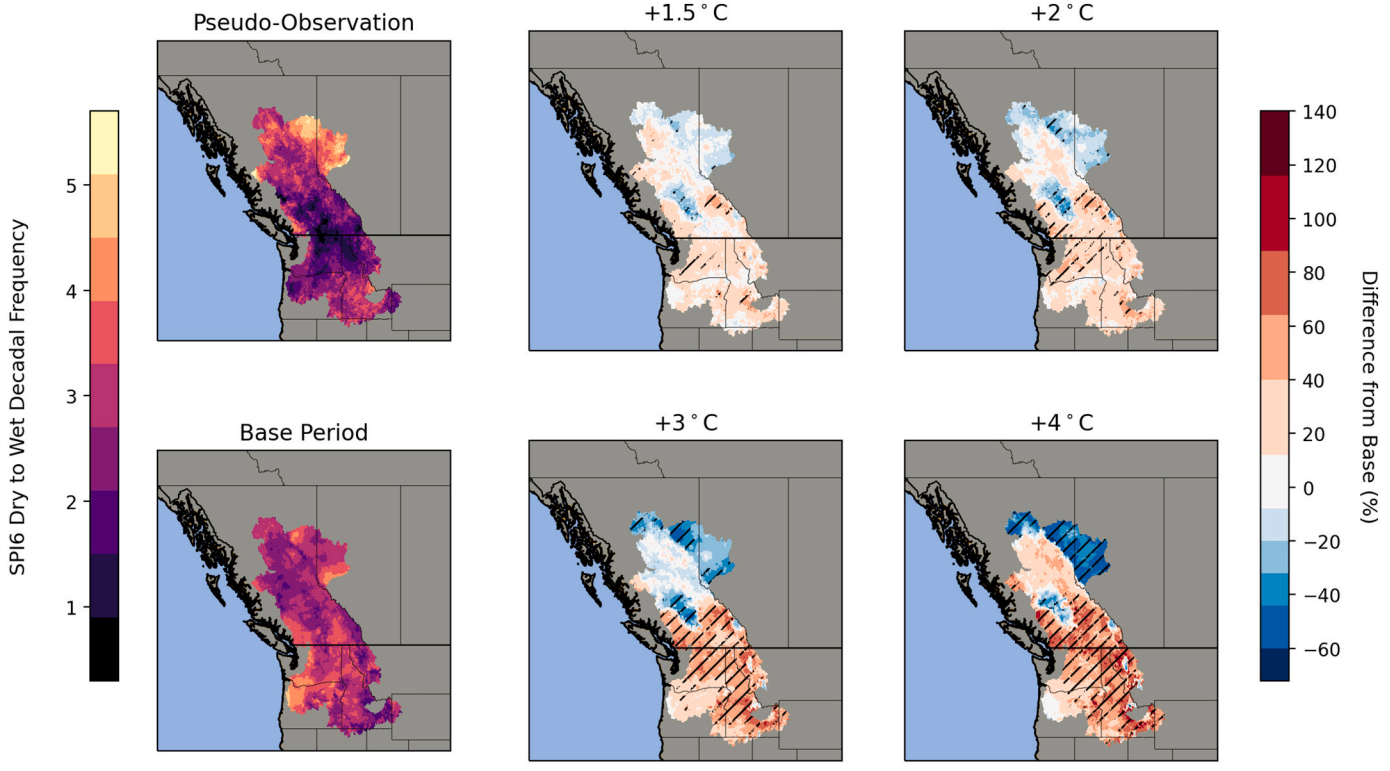

Fig. 5. Decadal frequency of CCEs over each warming period based on the gridded multi-model ensemble mean. Changes in future projections at different global warming levels are communicated as the percentage change relative to base period. Hatches show where the differences were significantly different from the base period. Significance at ≥95% confidence was obtained from a two-sided *t*-test.

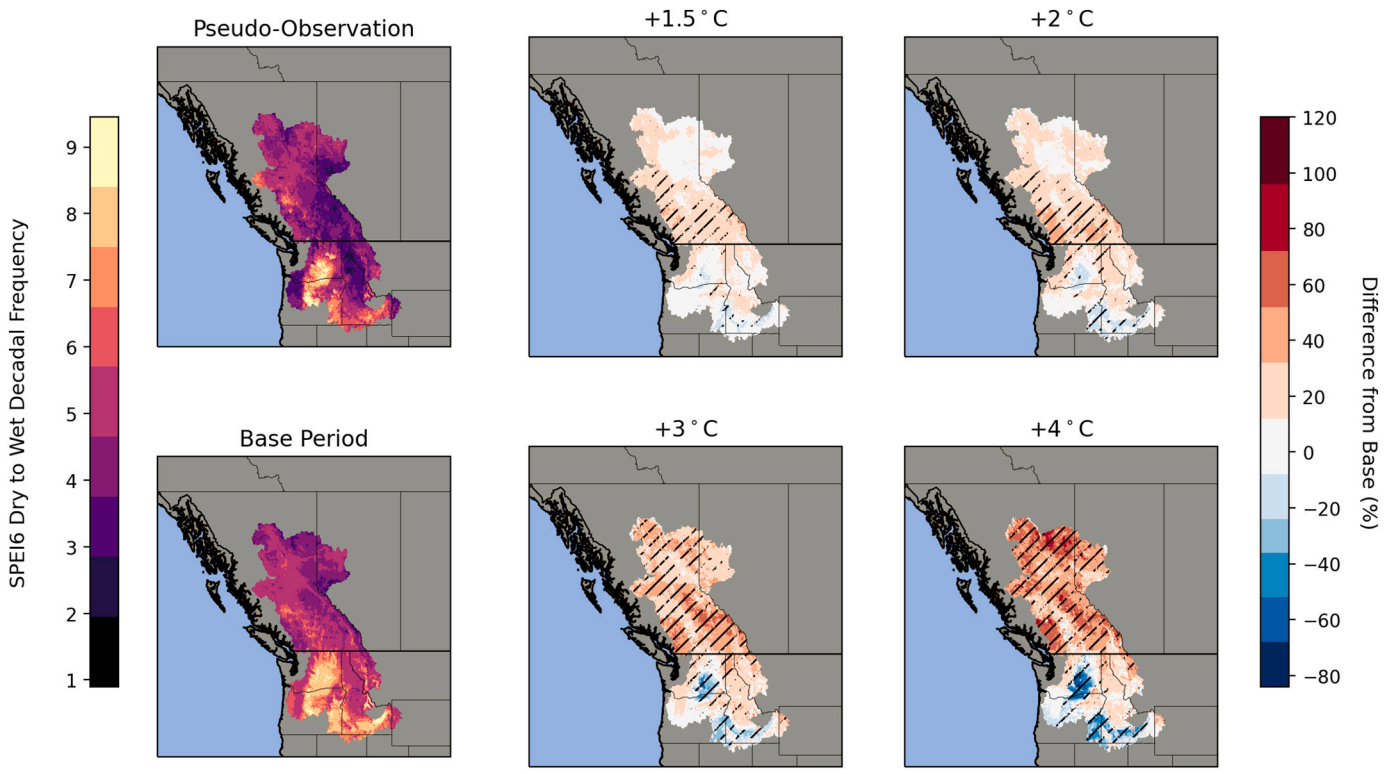

Fig. 6. Similar to Fig. 5, but for SPEI6.

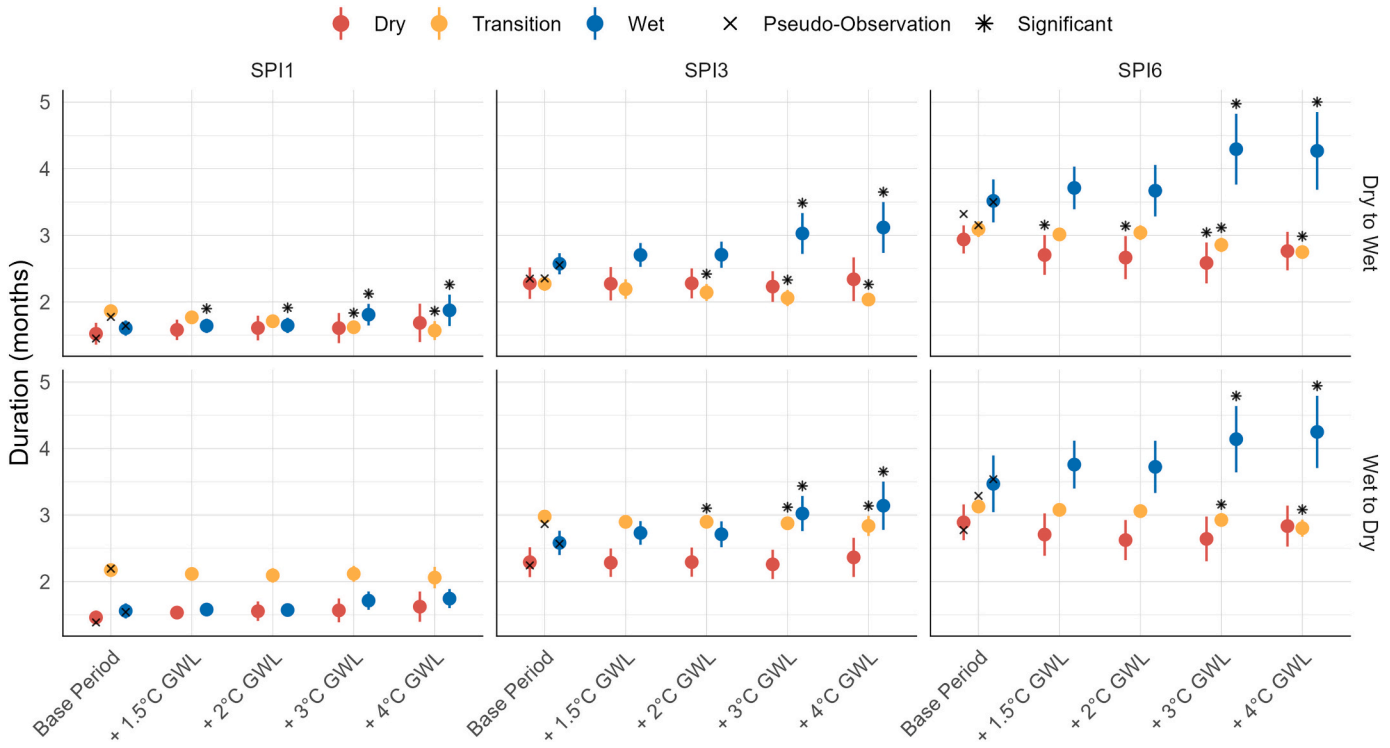

Fig. 7. Duration of wet and dry spells and transition time of CCEs (based on SPI). The points represent the multi-model average spatial mean and the bars show the ensemble standard deviation at each Global Warming Level (GWL). Significance at ≥95% confidence was obtained from a two-sided *t*-test.

northern Peace is expected to increase to 4 months (Fig. 9). On the contrary, transition time in some locations in southern Peace, eastern Fraser and central and southwest Columbia are projected to be 2 months at the 4 °C global warming level (Fig. 9). Although projected transition times based on SPI6 do not suggest abrupt transitions anywhere in the study area, some parts in the west and south Peace, as well as western and central Fraser and northern Columbia are projected to experience abrupt transitions as SPI1 results indicate (Fig. S11). However, there is

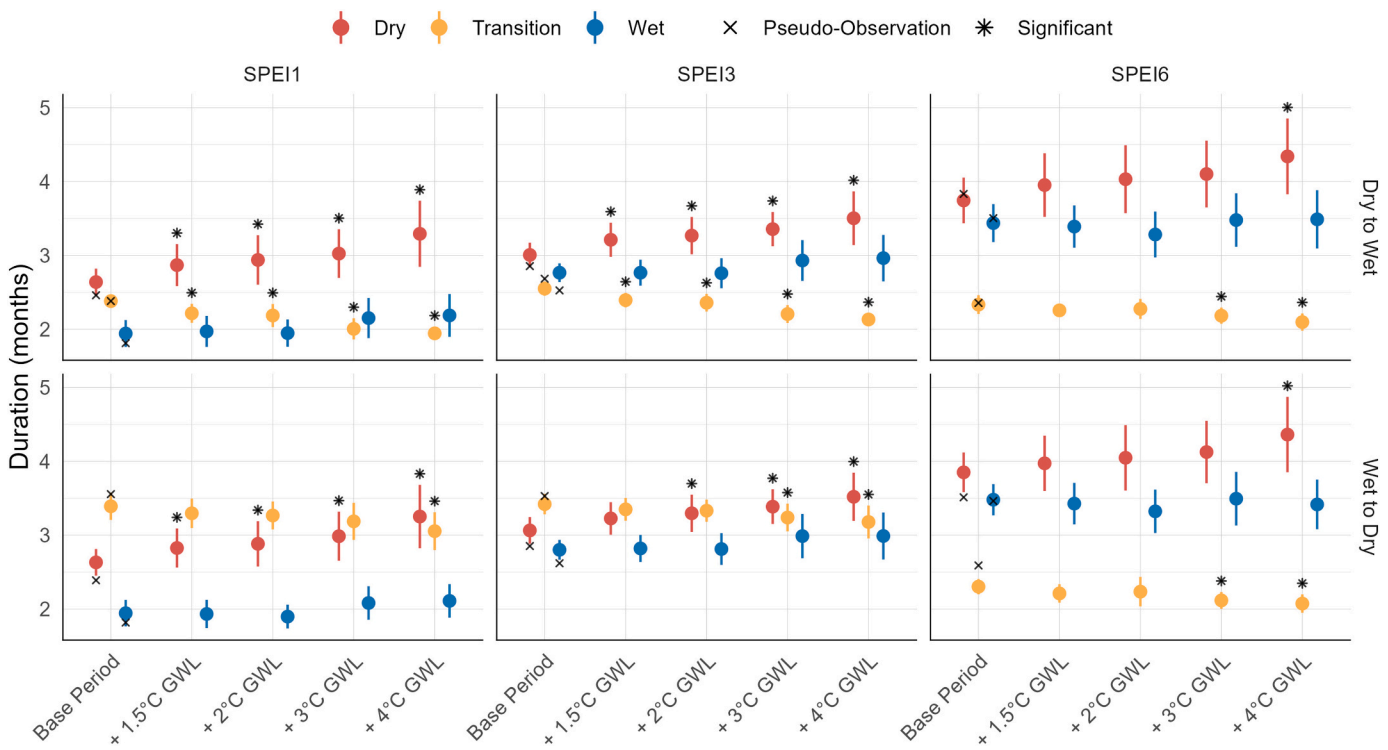

Fig. 8. Similar to Fig. 7 but for SPEI.

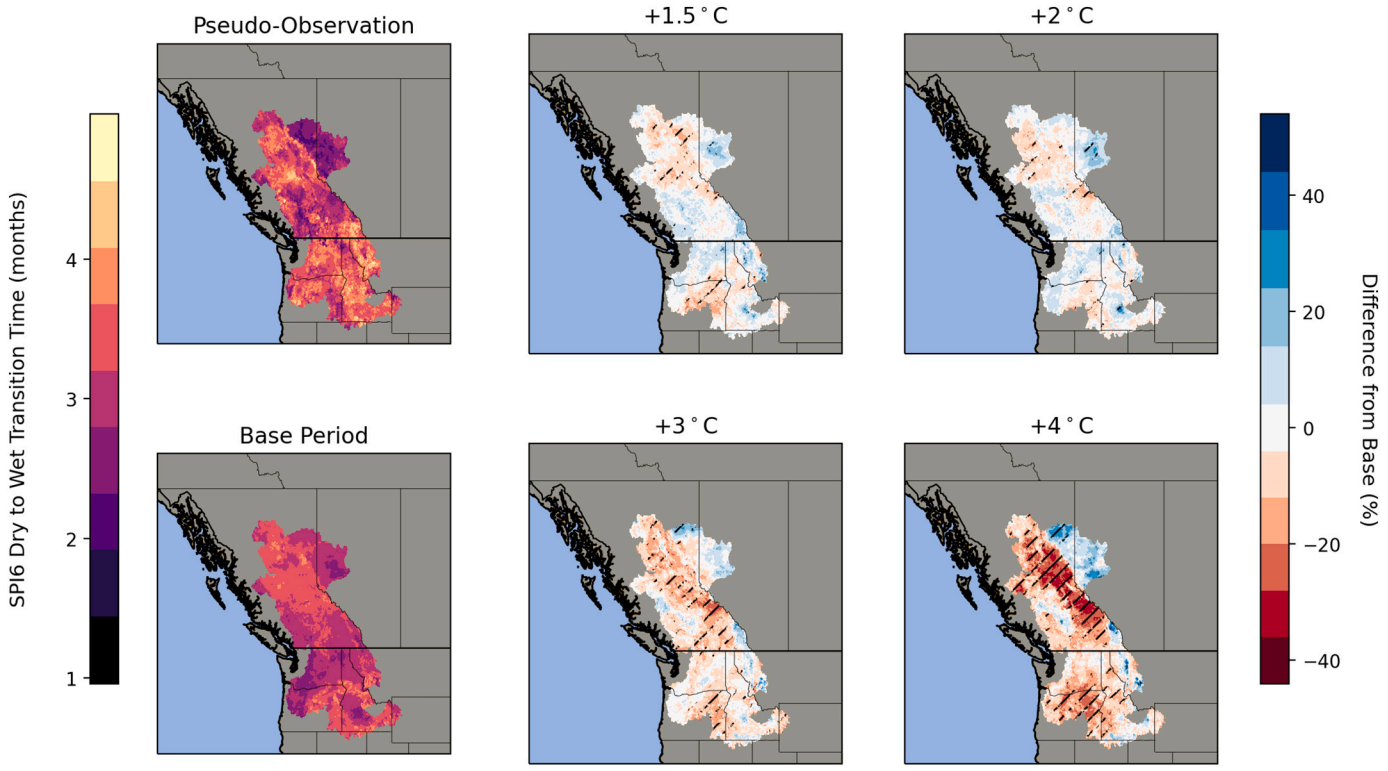

Fig. 9. Climatology of SPI6 dry-to-wet transition time. Maps show transition time in months over each warming period based on the multi-model ensemble mean. Changes in future projections at different global warming levels are communicated as the percentage change relative to base period. Hatches show where the differences were significantly different from the base period. Significance at ≥95% confidence was obtained from a two-sided *t*-test.

general agreement between SPI3 and SPI6 in the duration of transition time projected for different locations (Figs. S12 and S13). Results based on SPEI6 also indicate decreasing the transition time of CCEs to 2 months across the entire study area under climate change (Fig. 10). However, the transition time in the central part of Columbia is projected to increase to 4 to 5 months at the 4 °C global warming level (Fig. 10).

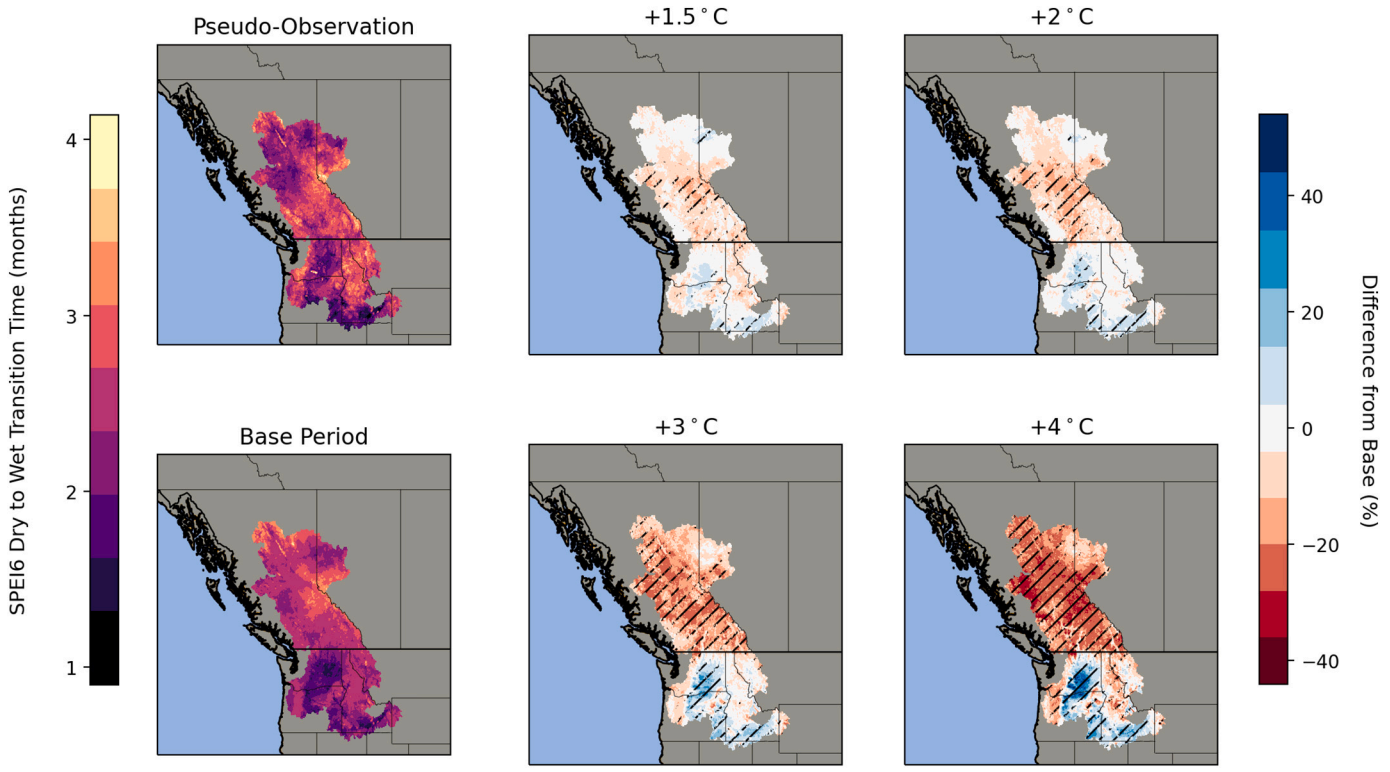

Fig. 10. Similar to Fig. 9, but for SPEI6.

Even though there are general agreements between SPEI6, SPEI1 and SPEI3 (Figs. S14, S15, and S16) in the projected length of transition time in different locations, future projections based on SPEI1 suggest abrupt transitions in the eastern Fraser basin near the Vancouver area at +3 °C GMT. Moreover, the western Peace, central and southwest and eastern Fraser, and northern Columbia are projected to experience abrupt drought to flood transitions at 4 °C global warming level (Fig. S14). Although the decreasing transition time is projected by both indices, the

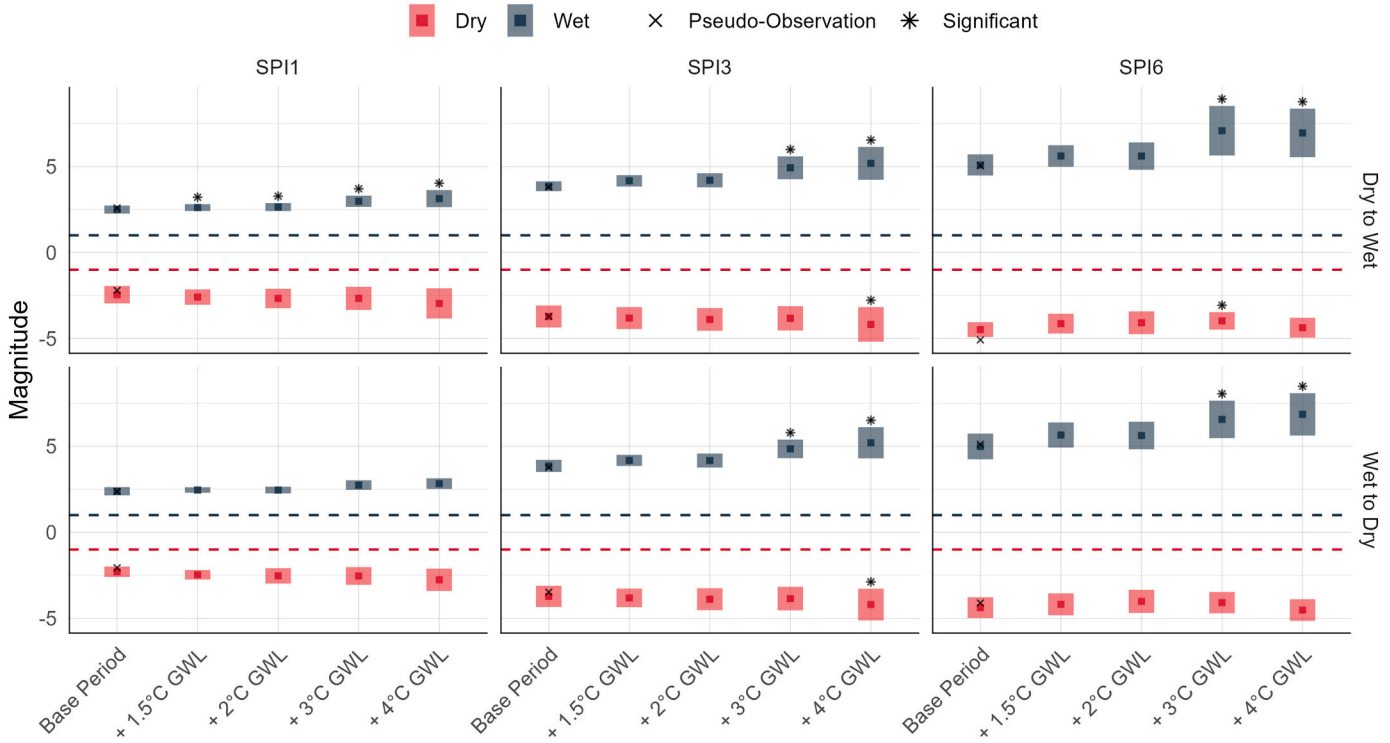

Fig. 11. Magnitude of wet and dry spells in CCEs based on SPI. The small rectangles show the multi-model average spatial mean and bars show the ensemble standard deviation. The dashed lines show the thresholds used to represent wet and dry spells in this study (±1). Significance at ≥95% confidence was obtained from a two-sided *t*-test.

projected transition time of CCEs is shorter by a month in most of the study areas based on SPEI compared to SPI.

4.3. Larger magnitudes of dry and wet spells in lagged compound events

The magnitude of wet and dry spells in CCEs at different warming levels is presented in Figs. 11 and 12 respectively based on SPI and SPEI. The figures show the multi-model average spatial mean and the ensemble standard deviation (see Figs. S19 and S20 for spatial variation of gridded ensemble mean). The results for the intensity of wet and dry spells are represented in Figs. S17 and S18.

The magnitude of both wet and dry spells in CCEs based on SPI is projected to increase under climate change (Fig. 11). Moreover, the intensity of both dry and wet spells based on SPI is projected to increase (Fig. S17). Magnitude can be influenced by the intensity and duration of the spells. Therefore, the projected increase in the magnitude of wet spells can be associated with the projected increases in the duration of wet spells as well as the intensification of both wet and dry spells in a warming future (Figs. 7 and 11, and Fig. S17). Further, the projected increases of dry spells magnitude in CCEs can be mostly due to the intensification of dry spells as the future projections of the ensemble mean based on SPI does not suggest considerable changes in the duration of the dry spells (Figs. 7 and 11, and Fig. S17).

In line with projections based on SPI, SPEI also indicates that the magnitude of both wet and dry spells in CCEs is projected to increase under climate change (Fig. 12). However, the increase is more noticeable in the magnitude of dry spells. Since the ensemble mean suggests increasing patterns in the duration of dry spells based on SPEI (Fig. 8) in a warming world, some part of the growth in the magnitude of dry spells in CCEs can be attributed to the changes in duration. However, dry spells in CCEs are projected to also intensify in a warmer world (Fig. S18). Therefore, increases in both the duration and intensity of dry spells can lead to growth in the magnitude of dry spells in CCEs. Intensification of future wet spells in CCEs is also projected by the ensemble mean. Since the projected changes in the duration of wet spells are not considerable, the projected pattern of increasing wet spell magnitudes in CCEs can be due to their intensification of them in a warming world (Figs. 8 and 12, and Fig. S18).

5. Discussion

The projections (Figs. 3 – 6) indicate an increasing pattern in the frequency of CCEs at different timescales under climate change. Short accumulation periods (1 and 3 months) can represent how climatic conditions can propagate to affect short-term soil moisture conditions. Therefore, less than normal precipitation or negative climatic water balance represented as dry spells can cause crop stress due to reduced short-term water availability. Further, the higher-than-normal precipitation and positive climatic water balance can lead to increased soil moisture, and therefore potentially increase the flood risk due to reduced infiltration capacity. A more frequent succession of such contrasting conditions can lead to vegetation diebacks (Moore, 2012). Furthermore, increasing the frequency of wet and dry spells accumulated at longer timescales (6 months) can enhance the chances of hydrologic floods and droughts, respectively. Therefore, more frequent successive floods and droughts that are probable in the future if global warming is not limited, could reduce the reliability of water resources for planning and management.

Our results indicate that the transition time of wet and dry spells is also projected to decrease (with statistically significant changes in many instances), which can pose challenges for water-resources management and emergency response. In addition to reservoir operation guidelines, the decision-making of reservoir operators can be influenced by experience and judgment as well, which can result in cognitive biases (Garcia et al., 2022). For instance, the flood of Brisbane in January 2011, (Australia's most expensive natural disaster to date) was caused not only by several days of intense rainfall but also by the flood operation decisions at the Wivenhoe and Somerset Dams (Garcia et al., 2022). This flood event occurred at the end of the decade-long Millennium drought, during which the dam operators struggled to meet water supply objectives and flood control was back of mind. Garcia et al. (2022) suggest the operators' recent experience with drought may have prompted them to

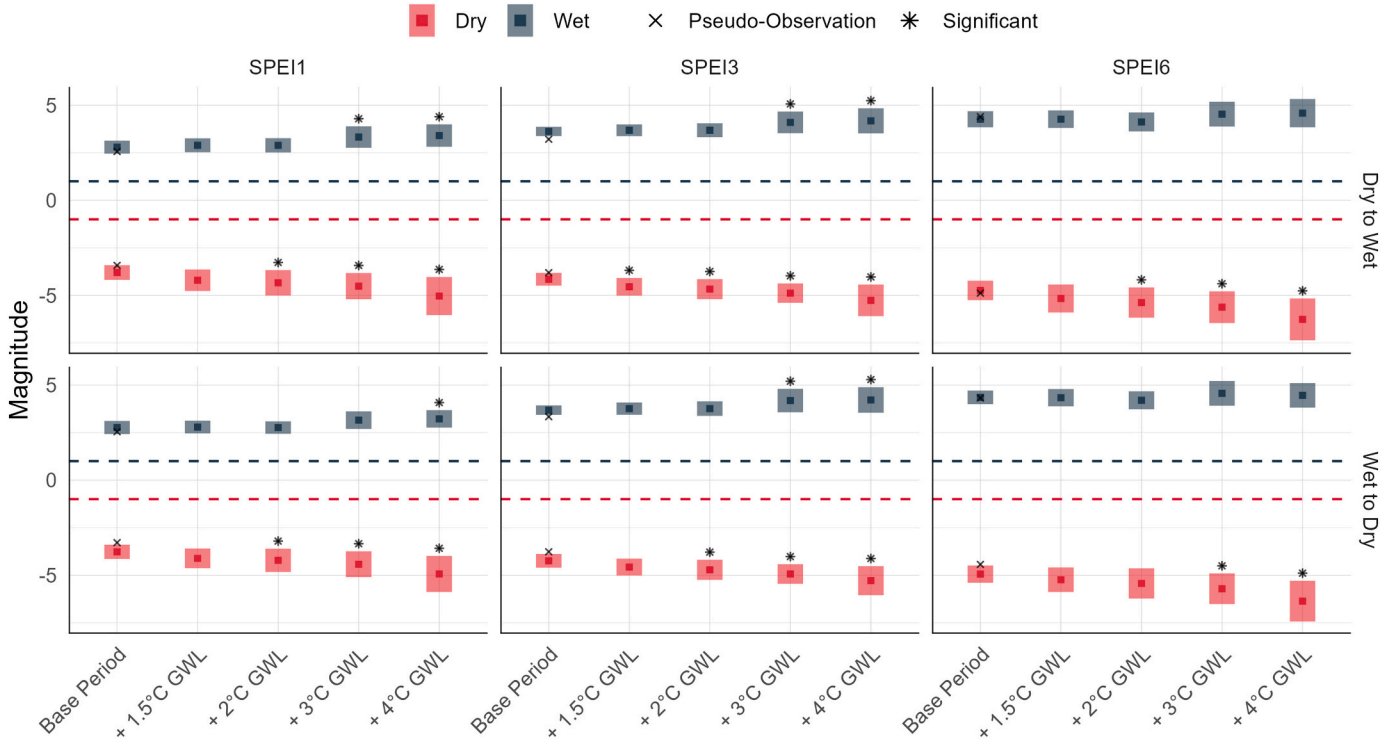

Fig. 12. Similar to Fig. 11, but based on SPEI.

underweight the risk of extreme flooding and over-weight the risk of water supply deficit. Moreover, the projected decrease in the transition times under climate change reduces the timespan over which actions to prepare for and cope with hazards. This reduces the recovery time and increases the failure probability of infrastructure and water demands.

Moreover, climate change can exacerbate the impacts of cognitive biases. While such biases are based on experience with historical conditions, the non-stationarity associated with climate change brings about unprecedented climatic situations. In addition, failure to detect, acknowledge, and manage such cognitive biases can create fragilities that can lead to catastrophic failures when extreme events occur. For instance, our multi-model ensemble projects change in the duration of the wet and dry spells (Figs. 7 – 10 and S9 – S16). Considering and incorporating such insights about the changing future characteristics of extreme events in reservoir operations and strategic planning for disaster risk reduction can limit the cognitive biases brought about by heuristics.

Coupled with the projected increase in the frequency of CCEs (Figs. 3 – 6), the variability of contrasting extreme precipitation alterations is projected to increase under climate change. The increased variability of the monthly (SPI1/SPEI1) CCEs (Figs. S3, S6, S11, and S14), reduces the predictability of these transitions which can challenge decision-making for water-resources managers. Moreover, increased variability of transitions between wet and dry spells accumulated over 3-months (Figs. S4, S7, S12, and S15) can put pressure on reservoir operations, decreasing the reliability of water supply, flood control and other reservoir benefits (Garcia et al., 2022). Due to the persistence of wet and dry spells on a longer timescale (SPI6/SPEI6), such abnormal (wet or dry) conditions can alter long-term patterns of water resources such as groundwater levels or streamflow (Figs. 3 – 10).

The future CCEs are projected to have larger magnitudes and intensify under climate change (Figs. 11, 12, and S17 – S20). Our findings of transitions between more intense wet and dry conditions are in line with the projections of Dong et al. (2018) that show intensified swing between wet and dry extremes in the sub-seasonal timescales. The increased dryness has been previously reported by the projections of Wartenburger et al. (2017) for many regions globally. Furthermore, the intensification of precipitation under climate change has been shown by Hartman et al., 2013. Moreover, this intensification of precipitation has been attributed to anthropogenic factors by Bindoff et al. (2013).

Our analysis shows some discrepancies when comparing the results based on SPI and SPEI. Results suggest that SPI can underestimate the risk of compound events as it overlooks how increasing temperatures could intensify regional water cycle. For example, the number of compound events captured by the SPEI is larger compared to the SPI. Moreover, results based on SPEI generally show shorter transition times (by a month over most of the study area) for CCEs compared to SPI. This difference implies that taking potential evapotranspiration (ultimately temperature) into account to identify the CCEs can more clearly represent the warming-induced intensification of the water cycle under climate change. There is theoretical evidence of water cycle acceleration brought about by rising surface temperature, which cause increases in evapotranspiration, and could result into faster atmosphere-land interchange (Huntington, 2006). Based on the Clausius-Clapeyron relation, the atmosphere can hold about 7% more water vapor for every degree Celsius it gets warmer (Bengtsson, 2010; Seager et al., 2010). Therefore, warmer air with higher evapotranspiration takes longer to get saturated potentially leading to longer dry spells and intensified drought conditions, and then has more water to release triggering heavy precipitation and corresponding severe floodings. Another reason is the increasing variabilities of precipitation and evapotranspiration (Lawrence et al., 2007). Higher evapotranspiration variability incurs a rapid rate of moving surface water from land to the atmosphere, contributing to the local transition from dry to wet periods (Qiu et al., 2021; Chen and Wang, 2022). Additionally, recent studies assessing droughts have found that it is not enough to monitor only precipitation, but the variables reflecting the change in evapotranspiration should be involved (Labudová et al., 2017; Paulo et al., 2012; Pei et al., 2017; Potop, 2011; Stagge et al., 2015). Therefore, we not only include the SPI but also the SPEI in our analysis as the SPEI can account for the possible effects of temperature variability and temperature extremes beyond the context of global warming.

It is difficult to explain the projected changes in the characteristic of lagged compound wet and dry spells from a physical standpoint, due to the complexity and variability of the mechanism causing the drivers of each component (wet and dry spells) of such compound events. This makes understanding lagged compound wet and dry spell events to be case-dependent, which can be influenced by climate variability, as well as climate change (He and Sheffield, 2020). Detailed analysis of individual event occurrences can reveal the synoptic conditions favourable for such compound event occurrences, especially since Maxwell et al. (2013 & 2017) have shown different storm types can cause such events in the same location. However, some of the projected patterns for the hydroclimatic events under climate change can bring about increases in the frequency of lagged compound dry and wet spells. As explained in the introduction, more frequent dry and wet spells are projected under global warming, which can increase the chances of successive contrasting hydroclimatic events. Warming can also change global climate variability such as El Nino/La Nina (Yu et al., 2017), or Arctic sea ice volume and extent (Francis et al., 2017), which can bring more year-to-year variability or persistence to weather patterns and influence regional precipitation and temperature anomalies (He, 2019). Therefore, we recommend investigating possible teleconnections of lagged compound wet and dry events with the large-scale modes of climate variability that impact the study area can improve the predictability of these compound events.

6. Conclusions

Hydroclimatic extremes (floods and droughts) have significant socio-economic and environmental impacts and are expected to become more variable under anthropogenic climate change. Recently, an upsurge in the temporal swings between the two contrasting extremes has been observed in several regions around the world, which has raised concerns about the increasing variability and rapid transitions between hydroclimatic extremes and their associated compounding economic and environmental impacts. In this study, we characterized lagged compound dry and wet spells and assessed the regional patterns of their characteristics at +1.5 to +4 °C global warming levels compared to the pre-Industrial era in Northwest North America. To this end, the Standardised Precipitation Index and Standardised Precipitation Evapotranspiration Index were used to find the wet and dry spells accumulated over different timescales (1, 3, and 6 months). The indices were calculated based on the simulated precipitation by an ensemble of downscaled and bias-corrected Global Climate Models consisting of 6 members and two medium and high emission scenarios. Moreover, the output evapotranspiration of the Variable Infiltration Capacity hydrologic model was used. Our results indicate that the frequency of both types of compound dry and wet spells (dry-to-wet and wet-to-dry) are projected to increase in a warming world. However, the study area is more prone to dry-to-wet compound events. In addition, the duration of dry and wet spells is expected to increase, whereas transitions between dry and wet spells are projected to occur more swiftly. Furthermore, future projections of our multi-model ensemble suggest larger magnitudes for both wet and dry spells that occur successively, which can be attributed to the projected increases in their durations as well their intensification. We also identified future spatial hotspots for each of these characteristics. The results assert that using SPI, which does not consider the impact of temperature underestimates the risk of such compound events. These findings highlight the importance of integrating compound wet-dry events into Disaster Risk Reduction strategies over the study area since the area is prone to such compound events and the vulnerability is

projected to increase under climate change.

CRediT authorship contribution statement

Reza Rezvani: Conceptualization, Data curation, Formal analysis, Investigation, Methodology, Writing – original draft, Visualization. **Wooyoung Na:** Conceptualization, Formal analysis, Investigation, Methodology, Writing – review & editing. **Mohammad Reza Najafi:** Conceptualization, Formal analysis, Investigation, Supervision, Project administration, Writing – review & editing.

Declaration of Competing Interest

The authors declare that they have no known competing financial interests or personal relationships that could have appeared to influence the work reported in this paper.

Data availability

Data will be made available on request.

Acknowledgement

Funding for this project is provided by the National Research Council Canada.

Appendix A. Supplementary data

Supplementary data to this article can be found online at https://doi.org/10.1016/j.atmosres.2023.106799.

References

Ansari, R., Grossi, G., 2022. Spatio-temporal evolution of wet–dry event features and their transition across the Upper Jhelum Basin (UJB) in South Asia. Nat. Hazards Earth Syst. Sci. 22 (2), 287–302. https://doi.org/10.5194/nhess-22-287-2022.

Beguería, S., Vicente-Serrano, S.M., Reig, F., Latorre, B., 2014. Standardized precipitation evapotranspiration index (SPEI) revisited: parameter fitting, evapotranspiration models, tools, datasets and drought monitoring. Int. J. Climatol. 34 (10), 3001–3023.

Bengtsson, L., 2010. The global atmospheric water cycle. Environmental Research Letters 5 (2), 025202.

Bindoff, N.L., Stott, P.A., AchutaRao, K.M., Allen, M.R., Gillett, N., Gutzler, D., Hansingo, K., Hegerl, G., Hu, Y., Jain, S., Mokhov, I.I., Overland, J., Perlwitz, J., Sebbari, R., Zhang, X., 2013. Detection and attribution of climate change: from global to regional. In: Stocker, T.F., Qin, D., Plattner, G.-K., Tignor, M., Allen, S.K., Boschung, J., Nauels, A., Xia, Y., Bex, V., Midgley, P.M. (Eds.), Climate Change 2013: The Physical Science Basis. Contribution of Working Group I to the Fifth Assessment Report of the Intergovernmental Panel on Climate Change. Cambridge University Press, Cambridge, United Kingdom and New York, NY, USA.

Bush, E., Lemmen, D.S., 2019. Canada's Changing Climate Report. https://doi.org/10.4095/314614.

Cannon, A.J., 2015. Selecting GCM scenarios that span the range of changes in a multimodel ensemble: application to CMIP5 climate extremes indices*. J. Clim. 28 (3), 1260–1267. https://doi.org/10.1175/JCLI-D-14-00636.1.

Cannon, A.J., Sobie, S.R., Murdock, T.Q., 2015. Bias correction of GCM precipitation by quantile mapping: how well do methods preserve changes in quantiles and extremes? J. Clim. 28 (17), 6938–6959. https://doi.org/10.1175/JCLI-D-14-00754.1.

Chegwidden, O.S., Nijssen, B., Rupp, D.E., Arnold, J.R., Clark, M.P., Hamman, J.J., Kao, S., Mao, Y., Mizukami, N., Mote, P.W., Pan, M., Pytlak, E., Xiao, M., 2019. How do modeling decisions affect the spread among hydrologic climate change projections? Exploring a large ensemble of simulations across a diversity of hydroclimates. Earth's Future 7 (6), 623–637. https://doi.org/10.1029/2018EF001047.

Chen, L., Ford, T.W., 2023. Future changes in the transitions of monthly-to-seasonal precipitation extremes over the Midwest in Coupled Model Intercomparison Project Phase 6 models. International Journal of Climatology 43 (1), 255–274.

Chen, H., Wang, S., 2022. Accelerated transition between dry and wet periods in a warming climate. Geophys. Res. Lett. 49 (19) https://doi.org/10.1029/2022gl099766.

Curry, C.L., Islam, S.U., Zwiers, F.W., Déry, S.J., 2019. Atmospheric rivers increase future flood risk in Western Canada's Largest Pacific River. Geophys. Res. Lett. 46 (3), 1651–1661. https://doi.org/10.1029/2018GL080720.

Dai, A., 2011. Drought under global warming: a review. Wiley Interdisciplinary Reviews: Climate Change 2 (1), 45–65.

Dibike, Y.B., Shrestha, R.R., Johnson, C., Bonsal, B., Coulibaly, P., 2021. Assessing climatic drivers of spring mean and annual maximum flows in western Canadian River Basins. Water 13 (12), 1617. https://doi.org/10.3390/w13121617.

Dong, L., Leung, L.R., Song, F., 2018. Future changes of subseasonal precipitation variability in North America during winter under global warming. Geophys. Res. Lett. 45 (22) https://doi.org/10.1029/2018GL079900.

Drumond, A., Stojanovic, M., Nieto, R., Gimeno, L., Liberato, M.L., Pauliquevis, T., Oliveira, M., Ambrizzi, T., 2021. Dry and wet climate periods over eastern South America: identification and characterization through the Spei Index. Atmosphere 12 (2), 155. https://doi.org/10.3390/atmos12020155.

Ford, T.W., Chen, L., Schoof, J.T., 2021. Variability and transitions in precipitation extremes in the Midwest United States. J. Hydrometeorol. 22 (3), 533–545. https://doi.org/10.1175/JHM-D-20-0216.1.

Francis, J.A., Vavrus, S.J., Cohen, J., 2017. Amplified Arctic warming and mid-latitude weather: new perspectives on emerging connections. Wiley's Clim. Change 8, 1–11.

Garcia, M., Yu, D., Park, S., Yousefi Bahambari, P., Mohajer Iravanloo, B., Sivapalan, M., 2022. Weathering water extremes and cognitive biases in a changing climate. Water Security 15, 100110. https://doi.org/10.1016/j.wasec.2022.100110.

Gillett, N.P., Cannon, A.J., Malinina, E., Schnorbus, M., Anslow, F., Sun, Q., Kirchmeier-Young, M., Zwiers, F., Seiler, C., Zhang, X., Flato, G., Wan, H., Li, G., Castellan, A., 2022. Human influence on the 2021 British Columbia floods. Weather Clim. Extremes 36, 100441. https://doi.org/10.1016/j.wace.2022.100441.

Gurrapu, S., Sauchyn, D.J., Hodder, K.R., 2022. Assessment of the hydrological drought risk in Calgary, Canada using weekly river flows of the past Millennium. J. Water Clim. Change 13 (4), 1920–1935. https://doi.org/10.2166/wcc.2022.348.

Hausfather, Z., Marvel, K., Schmidt, G.A., Nielsen-Gammon, J.W., Zelinka, M., 2022. Climate simulations: recognize the 'hot model'problem. Nature 605 (7908), 26–29.

He, X., 2019. Droughts and Floods in a Changing Environment Natural Influences, Human Interventions, ands Policy Implications, 228.

He, X., Sheffield, J., 2020. Lagged compound occurrence of droughts and pluvials globally over the past seven decades. Geophys. Res. Lett. 47 (14) https://doi.org/10.1029/2020GL087924.

Herring, S.C., Hoerling, M.P., Kossin, J.P., Peterson, T.C., Stott, P.A., 2015. Explaining Extreme Events of 2014 from a Climate Perspective, p. 180.

Hirabayashi, Y., Mahendran, R., Koirala, S., Konoshima, L., Yamazaki, D., Watanabe, S., Kim, H., Kanae, S., 2013. Global flood risk under climate change. Nat. Clim. Chang. 3 (9), 816–821. https://doi.org/10.1038/nclimate1911.

Hirsch, A.L., Wilhelm, M., Davin, E.L., Thiery, W., Seneviratne, S.I., 2017. Can climate-effective land management reduce regional warming? J. Geophys. Res. Atmos. 122 (4), 2269–2288. https://doi.org/10.1002/2016jd026125.

Huntington, T.G., 2006. Evidence for intensification of the global water cycle: Review and synthesis. J. Hydrol. 319 (1–4), 83–95.

Jalili Pirani, F., Najafi, M.R., 2020. Recent trends in individual and multivariate compound flood drivers in Canada's coasts. Water Resour. Res. 56 (8), e2020WR027785.

Jalili Pirani, F., Najafi, M.R., 2022. Multivariate analysis of compound flood hazard across Canada's Atlantic, Pacific and Great Lakes Coastal areas. Earth's Future 10 (8), e2022EF002655.

Kchouk, S., Melsen, L.A., Walker, D.W., van Oel, P.R., 2022. A geography of drought indices: Mismatch between indicators of drought and its impacts on water and food securities. Nat. Hazards Earth Syst. Sci. 22 (2), 323–344. https://doi.org/10.5194/nhess-22-323-2022.

Labudová, L., Labuda, M., Takáč, J., 2017. Comparison of SPI and SPEI applicability for drought impact assessment on crop production in the Danubian Lowland and the East Slovakian Lowland. Theor. Appl. Climatol. 128, 491–506.

Lawrence, D.M., Thornton, P.E., Oleson, K.W., Bonan, G.B., 2007. The partitioning of evapotranspiration into transpiration, soil evaporation, and canopy evaporation in a GCM: Impacts on land–atmosphere interaction. J. Hydrometeorol. 8 (4), 862–880.

Leonard, M., Westra, S., Phatak, A., Lambert, M., van den Hurk, B., McInnes, K., Risbey, J., Schuster, S., Jakob, D., Stafford-Smith, M., 2014. A compound event framework for understanding extreme impacts. WIREs Clim. Change 5 (1), 113–128. https://doi.org/10.1002/wcc.252.

Madakumbura, G.D., Kim, H., Utsumi, N., Shiogama, H., Fischer, E.M., Seland, Ø., Oki, T., 2019. Event-to-event intensification of the hydrologic cycle from 1.5 C to a 2 C warmer world. Scientific Reports 9 (1), 3483.

Mahmoudi, M.H., Najafi, M.R., Singh, H., Schnorbus, M., 2021. Spatial and temporal changes in climate extremes over northwestern North America: the influence of internal climate variability and external forcing. Clim. Chang. 165 (1–2), 14. https://doi.org/10.1007/s10584-021-03037-9.

Maxwell, J.T., Ortegren, J.T., Knapp, P.A., Soulé, P.T., 2013. Tropical cyclones and drought Amelioration in the Gulf and Southeastern Coastal United States. J. Clim. 26 (21), 8440–8452. https://doi.org/10.1175/JCLI-D-12-00824.1.

Maxwell, J.T., Knapp, P.A., Ortegren, J.T., Ficklin, D.L., Soulé, P.T., 2017. Changes in the mechanisms causing rapid drought cessation in the Southeastern United States. Geophys. Res. Lett. 44 (24) https://doi.org/10.1002/2017GL076261.

McKee, T.B., Doesken, N.J., Kleist, J., 1993. The Relationship of Drought Frequency and Duration to Time Scales, p. 6.

Moore, G.M., 2012. Flooding following a Drought: A Swift and Subtke Killer of Stressed Trees. University of Melbourne, pp. 1–13.

Moss, R., Intergovernmental Panel on Climate Change (Eds.), 2008. Towards New Scenarios for Analysis of Emissions, Climate Change, Impacts, and Response Strategies: IPCC Expert Meeting Report: 19–21 September, 2007, Noordwijkerhout. The Netherlands, Intergovernmental Panel on Climate Change.

Mount, J., Gray, B., Chappelle, C., Gartrell, G., Grantham, T., Moyle, P., Seavy, N., Szeptycki, L., 2017. Managing California's Freshwater Ecosystems: Lessons from the 2012-16 Drought. 54.

Mukherjee, S., Mishra, A.K., 2021. Increase in compound drought and heatwaves in a warming world. Geophys. Res. Lett. 48 (1) https://doi.org/10.1029/2020GL090617.
Najafi, M.R., Zwiers, F., Gillett, N., 2017. Attribution of the observed spring snowpack decline in British Columbia to anthropogenic climate change. J. Clim. 30 (11), 4113–4130.
Parry, S., 2019. Characterising Hydrological Drought Termination as a Basis for Improved Forecasting, p. 277.
Parry, S., Marsh, T., Kendon, M., 2013. 2012: from drought to floods in England and Wales. Weather 68 (10), 268–274. https://doi.org/10.1002/wea.2152.
Paulo, A.A., Rosa, R.D., Pereira, L.S., 2012. Climate trends and behaviour of drought indices based on precipitation and evapotranspiration in Portugal. Nat. Hazards Earth Syst. Sci. 12, 1481–1491.
Pei, T., Wu, X., Li, X., Zhang, Y., Shi, F., Ma, Y., Zhang, C., 2017. Seasonal divergence in the sensitivity of evapotranspiration to climate and vegetation growth in the Yellow River Basin, China. Journal of Geophysical Research: Biogeosciences 122 (1), 103–118.
Potop, V., 2011. Evolution of drought severity and its impact on corn in the Republic of Moldova. Theor. Appl. Climatol. 105, 469–483.
Qiu, L., Wu, Y., Yu, M., Shi, Z., Yin, X., Song, Y., Sun, K., 2021. Contributions of vegetation restoration and climate change to spatiotemporal variation in the energy budget in the loess plateau of china. Ecological Indicators 127, 107780.
Romolo, L., Prowse, T.D., Blair, D., Bonsal, B.R., Martz, L.W., 2006. The synoptic climate controls on hydrology in the upper reaches of the Peace River Basin. Part I: Snow accumulation. Hydrol. Process. 20 (19), 4097–4111.
Schnorbus, M., Werner, A., Bennett, K., 2010. Quantifying the Water Resource Impacts of Mountain Pine Beetle and Associated Salvage Harvest Operations across a Range of Watershed Scales: Hydrologic Modelling of the Fraser River Basin. Natural Resources Canada, Canadian Forest Service, Pacific Forestry Centre.
Schoeneberg, A.T., Schnorbus, M.A., 2021. Exploring the Strength and Limitations of PCIC's CMIP5 Hydrologic Scenarios, p. 42.
Seager, R., Naik, N., Vecchi, G.A., 2010. Thermodynamic and dynamic mechanisms for large-scale changes in the hydrological cycle in response to global warming. Journal of climate 23 (17), 4651–4668.
Seneviratne, S.I., et al., 2012. In: Field, C.B., et al. (Eds.), in Managing the Risks of Extreme Events and Disasters to Advance Climate Change Adaptation. Cambridge Univ. Press, pp. 109–230.
Shrestha, R.R., Cannon, A.J., Schnorbus, M.A., Alford, H., 2019. Climatic controls on future hydrologic changes in a subarctic River Basin in Canada. J. Hydrometeorol. 20 (9), 1757–1778. https://doi.org/10.1175/JHM-D-18-0262.1.
Seneviratne, S.I., Donat, M.G., Pitman, A.J., Knutti, R., Wilby, R.L., 2016. Allowable CO2 emissions based on regional and impact-related climate targets. Nature 529 (7587), 477–483. https://doi.org/10.1038/nature16542.
Seneviratne, S.I., Wartenburger, R., Guillod, B.P., Hirsch, A.L., Vogel, M.M., Brovkin, V., van Vuuren, Schaller, N., Boysen, L., Calvin, K.V., Doelman, J., Greve, P., Havlik, P., Humpenöder, F., Krisztin, T., Mitchell, D., Popp, A., Riahi, K., Rogelj, J., Stehfest, E., 2018. Climate extremes, land–climate feedbacks and land-use forcing at 1.5°C. Philosophical Transactions of the Royal Society A: Mathematical, Physical and Engineering Sciences 376 (2119), 20160450. https://doi.org/10.1098/rsta.2016.0450.
Sheffield, J., Wood, E.F., 2012. *Drought: past problems and future scenarios*. Routledge.
Shrestha, R.R., Bonsal, B.R., Bonnyman, J.M., et al., 2021. Heterogeneous snowpack response and snow drought occurrence across river basins of northwestern North America under 1.0°C to 4.0°C global warming. Clim. Chang. 164, 40. https://doi.org/10.1007/s10584-021-02968-7.
Singh, H., Pirani, F.J., Najafi, M.R., 2020. Characterizing the temperature and precipitation covariability over Canada. Theor. Appl. Climatol. 139 (3–4), 1543–1558. https://doi.org/10.1007/s00704-019-03062-w.
Shukla, S., Wood, A.W., 2008. Use of a standardized runoff index for characterizing hydrologic drought. Geophysical research letters 35 (2).
Singh, H., Najafi, M.R., Cannon, A.J., 2021. Characterizing non-stationary compound extreme events in a changing climate based on large-ensemble climate simulations. Clim. Dyn. 56 (5), 1389–1405.
Singh, H., Najafi, M.R., Cannon, A., 2022. Evaluation and joint projection of temperature and precipitation extremes across Canada based on hierarchical Bayesian modelling and large ensembles of regional climate simulations. Weather Clim. Extremes 36, 100443.
Skliris, N., Zika, J.D., Nurser, G., Josey, S.A., Marsh, R., 2016. Global water cycle amplifying at less than the clausius-clapeyron rate. Sci. Rep. 6 (1) https://doi.org/10.1038/srep38752.
Stagge, J.H., Tallaksen, L.M., Gudmundsson, L., Van Loon, Stahl, K., 2015. Candidate distributions for climatological drought indices (SPI and SPEI). International Journal of Climatology 35 (13), 4027–4040.
Swain, D.L., 2015. A tale of two California droughts: Lessons amidst record warmth and dryness in a region of complex physical and human geography: a tale of two california droughts. Geophys. Res. Lett. 42 (22) https://doi.org/10.1002/2015GL066628, 9999-10,003.
Swain, D.L., Horton, D.E., Singh, D., Diffenbaugh, N.S., 2016. Trends in atmospheric patterns conducive to seasonal precipitation and temperature extremes in California. Sci. Adv. 2 (4), e1501344 https://doi.org/10.1126/sciadv.1501344.
Swain, D.L., Langenbrunner, B., Neelin, J.D., Hall, A., 2018. Increasing precipitation volatility in twenty-first-century California. Nat. Clim. Chang. 8 (5), 427–433. https://doi.org/10.1038/s41558-018-0140-y.
Tam, B., Szeto, K., Bonsal, B., Flato, G., Cannon, A.J., Rong, R., 2018. CMIP5 drought projections in Canada based on the standardized precipitation evapotranspiration index. Can. Water Res. J. 44, 90–107.
Taylor, K.E., Stouffer, R.J., Meehl, G.A., 2012. An Overview of CMIP5 and the Experiment Design. Bull. Am. Meteorol. Soc. 93 (4), 485–498. Retrieved Dec 23, 2022, from. https://journals.ametsoc.org/view/journals/bams/93/4/bams-d-11-00094.1.xml. Retrieved Dec 23, 2022, from.
Vahedifard, F., AghaKouchak, A., Robinson, J.D., 2015. Drought threatens California's levees. Science 349 (6250), 799. https://doi.org/10.1126/science.349.6250.799-a.
Vahedifard, F., AghaKouchak, A., Ragno, E., Shahrokhabadi, S., Mallakpour, I., 2017. Lessons from the Oroville dam. Science 355 (6330), 1139–1140. https://doi.org/10.1126/science.aan0171.
Van Loon, A.F., 2013. On the Propagation of Drought: How Climate and Catchment Characteristics Influence Hydrological Drought Development and Recovery. Wageningen University.
Van Loon, A.F., 2015. Hydrological drought explained. WIREs. Water 2 (4), 359–392. https://doi.org/10.1002/wat2.1085.
Vicente-Serrano, S.M., Beguería, S., López-Moreno, J.I., 2010. A multiscalar drought index sensitive to global warming: the standardized precipitation evapotranspiration index. J. Clim. 23 (7), 1696–1718. Retrieved Dec 23, 2022, from. https://journals.ametsoc.org/view/journals/clim/23/7/2009jcli2909.1.xml. Retrieved Dec 23, 2022, from.
Vore, M.E., Déry, S.J., Hou, Y., Wei, X., 2020. Climatic influences on forest fire and mountain pine beetle outbreaks and resulting runoff effects in large watersheds in British Columbia, Canada. Hydrol. Process. 34 (24), 4560–4575. https://doi.org/10.1002/hyp.13908.
Wang, S.-Y.S., Yoon, J.-H., Becker, E., Gillies, R., 2017. California from drought to deluge. Nat. Clim. Chang. 7 (7), 465–468. https://doi.org/10.1038/nclimate3330.
Ward, P.J., de Ruiter, M.C., Mård, J., Schröter, K., Van Loon, A., Veldkamp, T., von Uexkull, N., Wanders, N., AghaKouchak, A., Arnbjerg-Nielsen, K., Capewell, L., Carmen Llasat, M., Day, R., Dewals, B., Di Baldassarre, G., Huning, L.S., Kreibich, H., Mazzoleni, M., Savelli, E., Wens, M., 2020. The need to integrate flood and drought disaster risk reduction strategies. Water Security 11, 100070. https://doi.org/10.1016/j.wasec.2020.100070.
Wartenburger, R., Hirschi, M., Donat, M.G., Greve, P., Pitman, A.J., Seneviratne, S.I., 2017. Changes in regional climate extremes as a function of global mean temperature: an interactive plotting framework. Geosci. Model Dev. 10 (9), 3609–3634. https://doi.org/10.5194/gmd-10-3609-2017.
Werner, A.T., Schnorbus, M.A., Shrestha, R.R., Eckstrand, H.D., 2013. Spatial and temporal change in the hydro-climatology of the Canadian portion of the Columbia River Basin under Multiple Emissions scenarios. Atmosphere-Ocean 51 (4), 357–379. https://doi.org/10.1080/07055900.2013.821400.
Werner, A.T., Schnorbus, M.A., Shrestha, R.R., Cannon, A.J., Zwiers, F.W., Dayon, G., Anslow, F., 2019. A long-term, temporally consistent, gridded daily meteorological dataset for northwestern North America. Sci. Data 6 (1), 180299. https://doi.org/10.1038/sdata.2018.299.
World Meteorological Organization (WMO), 2012. Standardized Precipitation Index: User Guidelines. World Meteorological Organization, pp. 1–24.
Yu, J.-Y., Wang, X., Yang, S., Paek, H., Chen, M., 2017. The changing El Niño-Southern oscillation and associated climate extremes. In: Wang, S.-Y.S., Yoon, J.-H., Funk, C. C., Gillies, R.R. (Eds.), Geophysical Monograph Series. John Wiley & Sons, Inc., pp. 1–38. https://doi.org/10.1002/9781119068020.ch1
Zargar, A., Sadiq, R., Naser, B., Khan, F.I., 2011. A review of drought indices. Environ. Rev. 19 (NA), 333–349. https://doi.org/10.1139/a11-013.
Zhou, S., Zhang, Y., Park Williams, A., Gentine, P., 2019. Projected increases in intensity, frequency, and terrestrial carbon costs of compound drought and aridity events. Sci. Adv. 5 (1), eaau5740 https://doi.org/10.1126/sciadv.aau5740.
Zscheischler, J., Martius, O., Westra, S., Bevacqua, E., Raymond, C., Horton, R.M., van den Hurk, B., AghaKouchak, A., Jézéquel, A., Mahecha, M.D., Maraun, D., Ramos, A. M., Ridder, N.N., Thiery, W., Vignotto, E., 2020. A typology of compound weather and climate events. Nat. Rev. Earth Environ. 1 (7), 333–347. https://doi.org/10.1038/s43017-020-0060-z.